Journal of Alzheimer's Disease 91 (2023) 779–794
DOI 10.3233/JAD-221046
IOS Press

Exposure to World Trade Center Dust Exacerbates Cognitive Impairment and Evokes a Central and Peripheral Pro-Inflammatory Transcriptional Profile in an Animal Model of Alzheimer's Disease

Ruth Iban-Arias[a,1], Kyle J. Trageser[a,1], Eun-Jeong Yang[a], Elizabeth Griggs[a], Aurelian Radu[a], Sean Naughton[a], Md Al Rahim[a], Oguchi Tatsunori[a], Urdhva Raval[a], Joshua Palmieri[a], Zerlina Huang[a], Lung-Chi Chen[b] and Giulio Maria Pasinetti[a,c,*]
[a]*Department of Neurology, Icahn School of Medicine at Mount Sinai, New York, NY, USA*
[b]*Department of Environmental Medicine, NYU Langone School of Medicine, New York, NY, USA*
[c]*Geriatrics Research, Education and Clinical Center, JJ Peters VA Medical Center, Bronx, NY, USA*

Accepted 4 November 2022
Pre-press 7 December 2022

Abstract.
Background: The terrorist attacks on September 11, 2001, on the World Trade Center (WTC) led to intense fires and a massive dense cloud of toxic gases and suspended pulverized debris. In the subsequent years, following the attack and cleanup efforts, a cluster of chronic health conditions emerged among First Responders (FR) who were at Ground Zero for prolonged periods and were repeatedly exposed to high levels of WTC particulate matter (WTCPM). Among those are neurological complications which may increase the risk for the development of Alzheimer's disease (AD) later in life.
Objective: We hypothesize that WTCPM dust exposure affects the immune cross-talking between the periphery and central nervous systems that may induce brain permeability ultimately promoting AD-type phenotype.
Methods: 5XFAD and wild-type mice were intranasally administered with WTCPM dust collected at Ground Zero within 72 h after the attacks. Y-maze assay and novel object recognition behavioral tests were performed for working memory deficits and learning and recognition memory, respectively. Transcriptomic analysis in the blood and hippocampus was performed and confirmed by RT qPCR.
Results: Mice exposed to WTCPM dust exhibited a significant impairment in spatial and recognition short and long-term memory. Furthermore, the transcriptomic analysis in the hippocampal formation and blood revealed significant changes in genes related to immune-inflammatory responses, and blood-brain barrier disruption.
Conclusion: These studies suggest a putative peripheral-brain immune inflammatory cross-talking that may potentiate cognitive decline, identifying for the first time key steps which may be therapeutically targetable in future studies in WTC FR.

Keywords: Blood-brain barrier, Claudin-5, cognitive decline, MMP-9, neuroinflammation, World Trade Center particulate matter

[1]These authors contributed equally to this work.

*Correspondence to: Giulio Maria Pasinetti, MD, PhD, Department of Neurology, Mount Sinai School of Medicine, 1 Gustave L. Levy Place, Box 1137, New York, NY 10029, USA. Tel.: +1 212 241 7938; Fax: +1 212 876 9042; E-mail: giulio.pasinetti@mssm.edu.

INTRODUCTION

The terrorist attacks on September 11, 2001, led the Twin Towers and Building 7 of the World Trade Center (WTC) in New York City to collapse resulting in intense fires and a massive dense cloud of toxic gases and suspended pulverized debris. Fires continued intermittently for 3 months after 9/11. During the aftermath, approximately 73,000 individuals were involved in the initial emergency response, rescue efforts, and clean-up. The World Trade Center Health Program (WTCHP) emerged after the catastrophe to monitor and treat first responders, including firefighters and emergency medical staff, general responders, including volunteers, and survivors suffering from 9/11-derived health conditions [1].

Immediately after the collapse of the WTC buildings, clouds of pollutants and toxins persisted for months including particles of different natures and sizes. Samples of settled dust from Ground Zero were collected during September 12-13, 2001 to analyze its composition and anticipate the potential human health impact [2–4]. Several pollutants including neurotoxins, asbestos, multiple chemical elements, as well as organic compounds such as polycyclic aromatic hydrocarbons (PAHs), and pesticides, most of them carcinogenic, were described in the WTCPM dust [5–8]. Many of these components have been shown to initiate or propagate inflammatory responses and may have deleterious effects on brain function [9].

Clinical follow-up of the WTC First Responders (FR) revealed epidemiological evidence suggesting that people exposed to high levels of WTCPM have seen their health negatively impacted, underlying an important public health burden. Initial studies of the longitudinal effects of WTCPM have largely investigated in relation to cardiovascular [10, 11], respiratory disorders [12–14], and cancer [15].

Nevertheless, as this cohort has begun to age, questions regarding the long-term effects of WTCPM exposure and the resultant neurological complications have been posed. Initial studies have correlated chronic exposure to WTCPM with neurologic and psychiatric disorders [16]. Clouston et al. [17] reported that chronic exposure to airborne dust and smoke might have a detrimental effect on blood-brain barrier (BBB) permeability; a pathologic feature in various neurodegenerative diseases, including Alzheimer's disease and related dementias (ADRD) [18, 19].

There is evidence suggesting that WTCPM-exposed FR suffering from chronic posttraumatic stress disorder (PTSD) are 3 times more likely to develop mild cognitive impairment (MCI) than the healthy population [20]. Furthermore, PTSD symptoms in FR have been correlated with alteration in neurodegeneration plasma-based biomarkers including a higher amyloid-β ($A\beta)_{1\text{-}42}/A\beta_{1\text{-}40}$ ratio, reduced soluble Aβ, high soluble tau protein, and high neurofilament light compared to healthy non-exposed to WTC dust individuals [21]. The combination of PTSD and WTCPM dust inhalation has been also associated with increased levels of systemic pro-inflammatory and neuroinflammatory sequelae, leading to accelerated aging processes and cognitive decline [17]. Interestingly, FR acutely exposed to high levels of dust, and carrying the *APOE* ε4 allele (which confers susceptibility to AD) were more prone to develop MCI and severe PTSD [20]. Hence, the evidence supports the hypothesis that FR acutely exposed to WTCPM may be at higher risk of age-associated neurodegenerative disorders, including AD. However, there is a significant dearth of research based on the molecular mechanisms of how WTCPM affected these individuals.

In the present study, we show that acute exposure to WTCPM may accelerate cognitive deterioration and AD-type neuropathology in mice genetically modified to develop AD-type cognitive phenotype. In addition, our transcriptomic studies strongly support the evidence that acute exposure to WTCPM may trigger generalized immune inflammatory cascades which may underlie the collective pathophysiology being experienced by FR following exposure to WTCPM.

MATERIALS AND METHODS

Mouse model

Pathogen-free, female wild-type (WT) (C57BL/6J) (Strain #000664) and transgenic 5XFAD (B6.Cg-Tg(APPSwFlLon,PSEN1*M146L*L286V) 6799Vas/Mmjax) (Strain #034848-JAX), were purchased from the Jackson Laboratory Animals (Bar Harbor, ME, USA). All animals were housed in a temperature-controlled ($20 \pm 2^{\circ}$C) vivarium and maintained on a 12/12 h light/dark cycle. Food and water were available *ad libitum*. As the vast majority of the FR exposed to the dust were around 30 years of age, we decided to use the equivalent mouse age being of 20–24 weeks [22]. All procedures

were approved by the Institutional Animal Care and Use Committee of the Icahn School of Medicine at Mount Sinai. All animal experiments complied with the ARRIVE guidelines and were carried out in accordance with the U.K. Animals (Scientific Procedures) Act, 1986 and associated guidelines, EU Directive 2010/63/EU for animal experiments, or the National Research Council's Guide for the Care and Use of Laboratory Animals.

WTC dust preparation and administration

WTCPM samples

WTCPM used in this study was provided by Dr. Lung-Chi Chen, Professor at NYU Langone Health, Department of Environmental Medicine, and represents the only existing material on-site at Ground Zero, to which FR were repeatedly exposed in the critical initial 72 h. Particle sampling, sizing, and characterization have previously been described [2, 5–7]. The mass median aerodynamic diameter of WTCPM <53 was found to be 23 μm, with size distributions of 10–53 μm, 2.5-1 μm, or ≤2.5 μm diameters comprising 42, 0.5, and 1.5% of the total mass, respectively [3]. All WTC particle samples (10–53 μm size range) were kept at room temperature in airtight containers and away from potential light exposure. WTC dust was weighted at the specific concentration of 125 μg/50 μl/animal using sterile water as a vehicle, just prior to use. Samples were also sonicated for approximately 1 h before use.

WTCPM samples preparation and intranasal instillation

WTCPM 10–53 μm preparation was previously described by Hernandez et al. [23]. Briefly, WTCPM 10–53 μm was suspended in sterile water 1 h prior to the administration and sonicated for 1 h. Mice were anesthetized in a closed container containing Isoflurane (1–3% in oxygen) (Butler Schein, Dublin, OH). Once sedated to one breath per two seconds, mice were manually placed in a supine position at an approximately 45° angle, allowing for unobstructed intranasal delivery of suspended particles or vehicle. 25 μl of dust or vehicle were carefully instilled into each nostril for a total of 50 μl per mouse. All mice were exposed to repeated intranasal (IN) instillation of WTCPM 10–53 μm. For this, 125 μg/dose was selected to achieve exposure burdens calculated to reflect those faced by FR exposed to Ground Zero air levels. The selected dosing amount of 125 μl, frequency, and sacrifice time point, were derived from Hernández et al. [23, 24]. According to those studies, this dose was the most physiologically relevant for our studies, and a higher dose of WTCPM 10–53 μm in C57BL/6J mice led to a ceiling effect (possibly due to airway blockage) and increased lethality with repeated dosing in a short period of time.

The same authors described the human equivalent dosing calculations that were acquired using allometric body weight factors of 0.67 (BW0.67) and 0.75 (BW0.75), considering the weight ratios of 0.02–0.03 kg for mice and 50–70 kg for humans and taking into account the FR intermediate exposure to WTCPM 10–53 μm for an 8-h shift at Ground Zero which is on the order of ≈50 mg/kg. Across both genotypes (WT and 5XFAD) there were three experimental groups: high (HE), low (LE), and no (NE)-exposure group. HE mice were exposed to 125 μg of WTCPM 10–53 μm on three consecutive days for 3 weeks (with 4-day recovery between each round of exposures = 9 total exposures × 125 μg = 1.125 mg; based on 100% deposition efficiency due to IN instillation). LE mice were exposed to 125 μg of WTC dust on just three consecutive days in the first week, then the vehicle in each subsequent week (3 total exposures = 375 μg). NE mice received the vehicle in all nine exposures. While this level is below the one routinely used in other rodent studies, to reach a cumulative level of exposure comparable to that experienced by WTC FR, and to reduce the IN-induced death in mice, the animals were dosed with 125 μg dust/instillation.

Behavioral studies

Y-maze Spontaneous Alternation test

On days 22-23-post first exposure (PFE), mice were tested for working memory deficits using the Y-maze spontaneous alternation assay. WT and 5XFAD mice were placed at the start arm on a Y-shaped maze and allowed to explore all three arms freely for 10 min. The frequency of alternation among the three arms was recorded with a NIR camera and measured with ANY-maze™ tracking software (Stoelting Co., IL, USA. Version 5.1 Beta). Generally, mice have an innate tendency to explore the environment they have not recently visited. Spatial working short-term memory impairment in this assay is defined as behavior wherein a mouse re-enters the same arm(s) repeatedly and thus does not remember which arms have been explored.

Novel Object Recognition test (NOR)

On days 29-30-PFE, learning and recognition memory were assessed via novel object recognition tests (NOR). This test was performed 7 days after the Y-maze to allow the mice to rest. Each mouse was placed in a square chamber and allowed to habituate to the environment for 2 d (5 min/d) prior to the cognitive assessment. On Day 3 (29 days-PFE), mice were placed in the same enclosure with an addition of two objects (a salt shaker and a toy block) and given 10 min to investigate. The time spent with both objects was recorded with a NIR camera and measured with ANY-maze^{TM} tracking software (Stoelting Co., IL, USA. Version 5.1 Beta). Each mouse was then removed and returned to its cage. After 1 h (short-term memory/ learning acquisition) or 24 h (longer-term memory/consolidation and recall), the enclosure was prepared with a familiar object from previous trials and a novel object. Each mouse was again placed in the enclosure and allowed to explore. Cognitively intact mice display an innate tendency to spend a greater amount of time investigating the novel object rather than the familiar one. Thus, an animal that does not remember which object it has been exposed to previously will spend similar amounts of time exploring both objects. Potential learning and memory deficits are calculated using a Preference Index as defined by the following formula: [Time at novel object / (Time at novel object + Time at familiar object)] x 100 (%).

Sample preparation

Blood collection

To monitor blood-associated changes due to the WTC dust exposure, blood was collected at the end of the experiment, 2 weeks post-last exposure in female WT and 5XFAD mice, by retro-orbital sinus collection. Animals were anesthetized in a closed container containing Isoflurane (1–3% in oxygen) (Butler Schein, Dublin, OH). Once sedated, they are held by the back of the neck and the loose skin of the head is tightened to allow for immobilization. Standard heparinized micro-hematocrit capillary tubes are used. The tip of the capillary is placed at the medial canthus of the eye under the nictitating membrane. The sinus is punctured and blood enters the tubing by capillary action. 200–250 µl (1% of the animal's body weight) of blood was collected into tubes with K2EDTA (Cat#365974; BD Microtainer, NJ, USA), and kept on ice for 15 min. Afterward, samples were processed for transcriptomic analysis.

Brain collection

Brains were collected and rinsed in cold 1X PBS, and microdissection for the isolation of the hippocampus was performed. The hippocampus was dissected and processed for transcriptomic analysis. Total RNA was extracted from hippocampus tissue using TRIzol (Cat#15596026; Invitrogen, MA, USA) followed by RNeasy Mini Kit (Cat#74104; Qiagen, MD, USA) according to the manufacturer's instructions.

Enzyme-linked immunosorbent assay (ELISA)

To measure the levels of the two amyloid-β (Aβ) peptides namely $A\beta_{1\text{-}40}$ and $A\beta_{1\text{-}42}$ in the prefrontal cortex and hippocampus, ELISA was performed using mouse $A\beta_{40}$ (Cat#KMB3481; Invitrogen, MA, USA) and mouse $A\beta_{42}$ (Cat#KMB3441; Invitrogen, MA, USA) ELISA kits following the manufacturer's instructions. Briefly, frozen tissue samples were weighted and homogenized in a cold buffer, which consisted of 5 M guanidine-HCl/50 mM Tris supplemented with an inhibitor cocktail containing AEBSF (Cat#78431; Thermo Fisher, MA, USA). The samples were incubated using an orbital shaker for 3 h at room temperature and centrifuged at 16,000× *g* for 20 min. Subsequently, supernatants were collected and diluted with standard diluent buffer to an appropriate concentration. Standards and samples were incubated in $A\beta_{1\text{-}40}$ or $A\beta_{1\text{-}42}$ polyclonal antibody-precoated 96-well plates. Plates were read at 450 nm using a microplate reader (Varioskan^{TM} Lux; Thermo Fisher, MA, USA). Concentrations of $A\beta_{1\text{-}40}$ and $A\beta_{1\text{-}42}$ in the prefrontal cortex or hippocampus were calculated using the standard curves. The total amount of protein from each sample was normalized using the BCA assay (Cat#23225; Thermo Fisher, MA, USA).

Transcriptomic analysis

Multiplexed gene expression in the hippocampus and blood of WT and 5XFAD mice after WTC dust exposure was conducted using the Nanostring nCounter Mouse Neuropathology Panel (XT-CSO-MNROP1-12) and Immunology Panel (XT-CSO-MNROP1-12), respectively, in collaboration with the Quantitative PCR CoRE at the Icahn School of Medicine at Mount Sinai. Briefly, RNA was extracted from hippocampus homogenate and blood using a Direct-zol RNA Miniprep (Cat#R2051; Zymo Research, CA, USA) according to the manufacturer's instructions.

Transcriptional changes were analyzed using nSolver (Version 4.0), with additional downstream analyses performed using Ingenuity Pathway Analysis (IPA; Qiagen, Inc.). Analysis of cell populations by Nanostring cell score is calculated as the average log-scale expression of characteristic genes for specific cell populations as identified by nSolver.

Gene expression validation by quantitative RT qPCR

RNA obtained from mouse hippocampi was reverse transcribed using the High-Capacity cDNA Reverse Transcription Kit (Cat#4368813, Thermo Fisher, MA, USA) according to the manufacturer's instructions. 30–40 ng of RNA was used per reaction and yielded 2-3 μg/μl of DNA. Gene expression was measured in 3 replicates. The expression of *Nlrp3, Interferon-γ, Il-1β, Il-10, Nfκβ, Il-6, Tnf-α, Hmgb1, Il-18, GSDMD, Claudin-5, Vegfα, Itgam, Thy-1, Cx3cr1, PSD95, Mapk3, MMP9, MSR1, MIP-1α/CCL3* (Supplementary Table 1) was measured by Real-Time Quantitative Reverse Transcription PCR (RT qPCR) using Power SYBR Green PCR Master Mix (Cat# 4367659, Thermo Fisher, MA, USA) in an ABI PRISM 7900HT Sequence Detection System at the Icahn School of Medicine qPCR CoRE. Graphs represent fold change in cDNA values with respect to non-exposed controls normalized to hypoxanthine phosphoribosyltransferase (*Hprt*) internal control using the $2^{-\Delta\Delta Ct}$ method.

Brain tissue analysis by inductively coupled plasma-mass spectrometry (ICP-MS)

Brain hemispheres stored at –80°C were thawed and placed on watch glasses in a tissue culture hood. The watch glasses were previously cleaned with detergent, followed by 50% HCl (Cat#A466-1, Fisher Scientific) and 50% HNO_3 (Cat#A509P212, Thermo Scientific), for 1 h at 80°C. All brain samples were collected and homogenized using ceramic tools (X-Acto), to avoid any metal contamination. Two technical replicates were generated for each brain. Tissue was transferred to 30 ml Teflon bottles (Cat#02-923-30AA, Thermo Scientific), previously cleaned as the watch glasses. Three groups were created: control with no tissue, quality control, containing 25–50 mg of oyster tissue as the standard reference material (Cat#SRM 1566b, NIST), and sample with brain tissue. Bottles were weighed using an antistatic system (Zerostat –3 anti-static gun, MiltyPro) to neutralize electrostatic charges. Subsequently, tissue was dried in a microwave (1600 W) at 40% power in 2 sessions × 1 h with a 30 min-pause in between. Afterward, bottles were weighed to estimate the percentage of dry material. For trace elemental analysis, tissue was digested with 2 ml of HNO_3 (Cat#A467-1, Thermo Scientific), followed by 3 ml of HCl (Cat#A466-1, Fisher Scientific), in a heating block (120°C) for 2 h. As a final step, 1 ml of H_2O_2 (Cat#P170-500, Fisher Scientific) was added, and the bottle caps were replaced by a plastic cover, to allow for liquid evaporation, at 120°C. The content of the bottles was transferred to pre-cleaned 15 ml polystyrene tissue culture tubes and brought to a final volume of 10 ml with distilled H_2O (10% final acid content). The samples were analyzed at the Lamont-Doherty Earth Observatory of Columbia University (New York, USA) on a Thermo Element XR high-resolution ICP-MS. The concentration of elements was computed as ng per mg of wet brain tissue.

Statistical analysis

All values are expressed as the mean and standard error of the mean (S.E.M). One-way ANOVA with Tukey's posthoc was performed for overall comparisons. One-way ANOVA with Dunnett's multiple comparisons test was done to compare the control group to the test groups. T-test analysis (two-tails, equal variance) was used to compare two experimental groups. Outliers (2 S.E.M. from the mean) were removed from the analysis. Statistical analysis was performed using GraphPad Prism (version 9.1.1). Significant differences were set to $^{*}p \leq 0.05$, $^{**}p \leq 0.01$, $^{***}p \leq 0.001$, $^{****}p < 0.0001$.

RESULTS

WTC dust-exposed mice display spatial working memory impairment

Previous studies have identified a heightened incidence of cognitive dysfunction in WTC FR relative to non-exposed individuals, with impairments noted in reaction speed, processing speed, and memory [25]. We hypothesized that repeated exposure to WTCPM may directly affect the CNS, leading to memory dysfunction. To directly investigate the effects of WTCPM, exposure in mice genetically modified to develop AD-type phenotype and WT mice were administered intranasally with the dust for 3 consecutive days (125 μg/50 μl/animal/dose) for 3 weeks

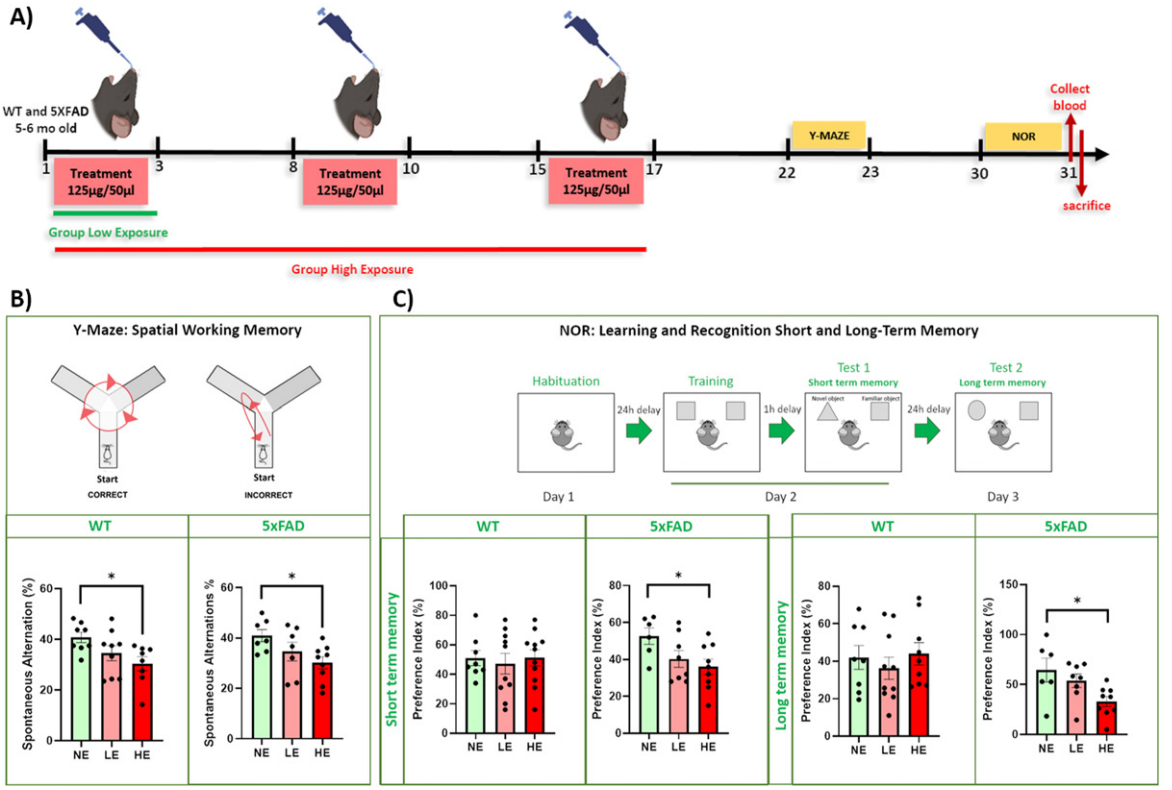

Fig. 1. A) WTCPM exposure paradigm. WT and 5XFAD mice were assigned to three experimental groups: high (HE), low (LE), and no (NE)-exposure group. HE mice were exposed to 125 µg of WTCPM 10–53 µm on three consecutive days for 3 weeks (with a 4-day recovery between each round of exposures. LE mice were exposed to 125 µg of WTC dust on just three consecutive days in the first week, then the vehicle in each subsequent week (3 total exposures = 375 µg). NE mice received the vehicle in all nine exposures. The following week memory and learning performance were measured using Y-maze and Novel Object Recognition (NOR). The day after blood was collected and animals were sacrificed for further analysis. B) Evaluation of spatial working memory measuring the frequency of alternation among the three arms using the Y-maze spontaneous alternation assay on days 22-23 PFE. Both WT and 5XFAD mice exhibited dose-dependent decreases in working memory after exposure to WTC dust, with only the HE group (mean ± S.E.M: WT: 30.35 ± 2.77; 5XFAD: 30.13 ± 2.40) displaying significant impairment compared to those animals not exposed to the dust (NE) (mean ± S.E.M: WT: 40.74 ± 2.015; 5XFAD: 40.92 ± 2.40) (NE versus LE: WT: *ns*, $p = 0.2401$; 5XFAD: *ns*, $p = 0.3120$; NE versus HE: WT: $^{*}p = 0.035$; 5XFAD: $^{*}p = 0.033$; LE versus HE: WT: *ns*, $p = 0.5076$; 5XFAD: *ns*, $p = 0.5037$). C) Learning acquisition and memory consolidation and recall in 5XFAD and WT exposed to WTC dust. Novel Object Recognition (NOR) task was performed 30-31 days PFE and preference Index measured. WT animals treated with low (mean ± S.E.M: 40.20 ± 7.03) and high (mean ± S.E.M: 51.18 ± 5.49) dust exposure, did not show significant differences in exploratory behavior onto the novel object compared to those non-exposed mice (mean ± S.E.M: 51.00 ± 5.11) (NE versus LE: *ns*, $p = 0.9055$; NE versus HE: *ns*, $p = 0.8796$). On the contrary, 5XFAD animals exposed to high doses of dust (mean ± S.E.M: 36.00 ± 4.15), showed significantly more preference to explore the familiar object rather than the novel when compared to no exposure mice, depicting underlying memory alteration, putatively due to dust exposure (mean ± S.E.M: 52.67 ± 4.49) (NE versus LE: *ns*, $p = 0.1715$; NE versus HE: $^{*}p = 0.045$). Long-term memory consolidation examined 24hrs after the second session. WT animals did not show any difference in exploratory preference among the three experimental groups (mean ± S.E.M: NE: 42.02 ± 6.35; LE: 36.27 ± 5.96; HE: 43.94 ± 6.03) (NE versus LE: *ns*, $p = 0.7883$; NE versus HE: *ns*, $p = 0.9748$). However, a significant dose-related decrease in memory consolidation was observed in 5XFAD, depicting a cognitive impairment and difficulty to recognize the familiar object (mean ± S.E.M: NE: 64.55 ± 11.92; LE: 53.67 ± 6.70; HE: 32.96 ± 4.98) (NE versus LE: *ns*, $p = 0.6022$; NE versus HE: $^{*}p = 0.0233$).

(Fig. 1A). After 2 weeks post-final exposure, the spatial working memory was examined using the Y-maze spontaneous alternation assay on days 22–23 post-final exposure (Fig. 1B).

The frequency of alternation among the three arms (in %) was evaluated. Both WT and 5XFAD mice exhibited dose-dependent decreases in working memory after exposure to WTC dust, with only the HE group (mean ± S.E.M: WT: 30.35 ± 2.77; 5XFAD: 30.13 ± 2.40) displaying significant impairment compared to those NE animals to the dust (mean ± S.E.M: WT: 40.74 ± 2.015; 5XFAD:

40.92 ± 2.40) (NE versus LE: WT: ns, $p = 0.2401$; 5XFAD: ns, $p = 0.3120$; NE versus HE: WT: $^{*}p = 0.035$; 5XFAD: $^{*}p = 0.033$; LE versus HE: WT: ns, $p = 0.5076$; 5XFAD: ns, $p = 0.5037$) (Fig. 1B). These results provide support to the hypothesis that repeated high dose of WTCPM dust exposure can be directly linked to working memory deficits that might persist for an extended period of time after the initial exposure.

Next, we assessed if learning acquisition and memory consolidation, and recall was affected by exposure to WTCPM. At ∼30 days PFE, 5XFAD, and WT mice were subjected to a Novel Object Recognition (NOR) task. 24 h after habituation to the apparatus, mice were presented with two identical objects to explore for 10 min, and after a 1-h intersession interval, one of the two objects was replaced by a novel and unfamiliar object. When the cognitive abilities are intact, the animals tend to explore the novel object due to innate motivation for novelty rather than familiarity, since they remember the familiar object. WT animals treated with low (mean ± S.E.M: 40.20 ± 7.03) and high (mean ± S.E.M: 51.18 ± 5.49) dust exposure, did not show significant differences in exploratory behavior onto the novel object compared to those non-exposed mice (mean ± S.E.M: 51.00 ± 5.11) (NE versus LE: ns, $p = 0.9055$; NE versus HE: ns, $p = 0.8796$). On the contrary, 5XFAD animals exposed to high doses of dust (mean ± S.E.M: 36.00 ± 4.15), showed significantly more preference to explore the familiar object rather than the novel when compared to no exposure mice, depicting underlying memory alteration, putatively due to dust exposure (mean ± S.E.M: 52.67 ± 4.49) (NE versus LE: ns, $p = 0.1715$; NE versus HE: $^{*}p = 0.045$).

Long-term memory consolidation was examined 24 h after the second session by replacing the novel object with a second new object. WT animals did not show any difference in exploratory preference among the three experimental groups (mean ± S.E.M: NE: 42.02 ± 6.35; LE: 36.27 ± 5.96; HE: 43.94 ± 6.03) (NE versus LE: ns, $p = 0.7883$; NE versus HE: ns, $p = 0.9748$) (Fig. 1C). However, a significant dose-related decrease in memory consolidation was observed in 5XFAD, depicting a cognitive impairment and difficulty to recognize the familiar object (mean ± S.E.M: NE: 64.55 ± 11.92; LE: 53.67 ± 6.70; HE: 32.96 ± 4.98) (NE versus LE: ns, $p = 0.6022$; NE versus HE: $^{*}p = 0.0233$) (Fig. 1C). These results provide support for our hypothesis that repeated high-level WTC dust exposure may have stronger effects on cognition, more specifically learning acquisition and memory consolidation, in animals that are genetically determined to develop AD-type Aβ pathology.

$A\beta_{42/40}$ levels increase in the prefrontal cortex following WTC dust exposure

Based on the evidence suggesting that cognitive deterioration is worsened by acute WTCPM exposure in mice genetically modified to develop AD-type phenotype we hypothesize that one potential mechanism of cognitive deterioration could be a manifestation of AD-Aβ neuropathology in the brain as in part also observed in FR [21]. Based on this and the evidence that AD-Aβ neuropathology has a key role in the onset of AD- cognitive deterioration, we next examined the effect of the WTCPM IN instillation of WTCPM dust on the levels of $A\beta_{1\text{-}42}$ and $A\beta_{1\text{-}40}$, in the prefrontal cortex and hippocampus of 6-7-month-old WT and 5XFAD mice.

We found a statistically significant and selective increase in the ratio $A\beta_{42/40}$, and index of amyloid-β protein precursor (AβPP) processing and AD-amyloid neuropathology) in non-exposed 5XFAD mice compared to non-exposed WT in the hippocampus (mean ± S.E.M: WT – dust: 15.82 ± 2.46; 5XFAD – dust: 30.58 ± 1.67; $^{***}p = 0.0004$). No detectable changes in $A\beta_{1\text{-}42/1\text{-}40}$ ratio was found in the prefrontal cortex (mean ± S.E.M: WT – dust: 20.10 ± 2.22; 5XFAD – dust: 39.67 ± 4.97; ns, $p = 0.073$) (Fig. 2). Interestingly, animals exposed to the dust (lowest dose) showed statistically significant differences for $A\beta_{1\text{-}42}$, $A\beta_{1\text{-}40}$ ratio compared to WT non-exposed only in the prefrontal cortex (mean ± S.E.M: 5XFAD + dust: 41.95 ± 5.85; WT– dust versus 5XFAD + dust: $^{*}p = 0.025$). However, no effect of WTCPM dust exposure was observed in the hippocampus compared to WT – dust (mean ± S.E.M: 5XFAD + dust: 19.70 ± 1.25; WT – dust versus 5XFAD + dust: ns, $p = 0.286$). No differences were observed in 5XFAD non-exposed and exposed to WTCPM dust in either brain region (prefrontal cortex: ns, $p = 0.948$; hippocampus: ns, $p = 0.061$) (Fig. 2). In addition, 5XFAD mice exposed to high levels of dust did not show significant differences compared to those exposed to low levels of dust (data not shown).

The resulting data for the $A\beta_{1\text{-}42/1\text{-}40}$ ratio reveals the potential effect of the WTCPM exposure in 5XFAD mice, on the changes in Aβ levels being

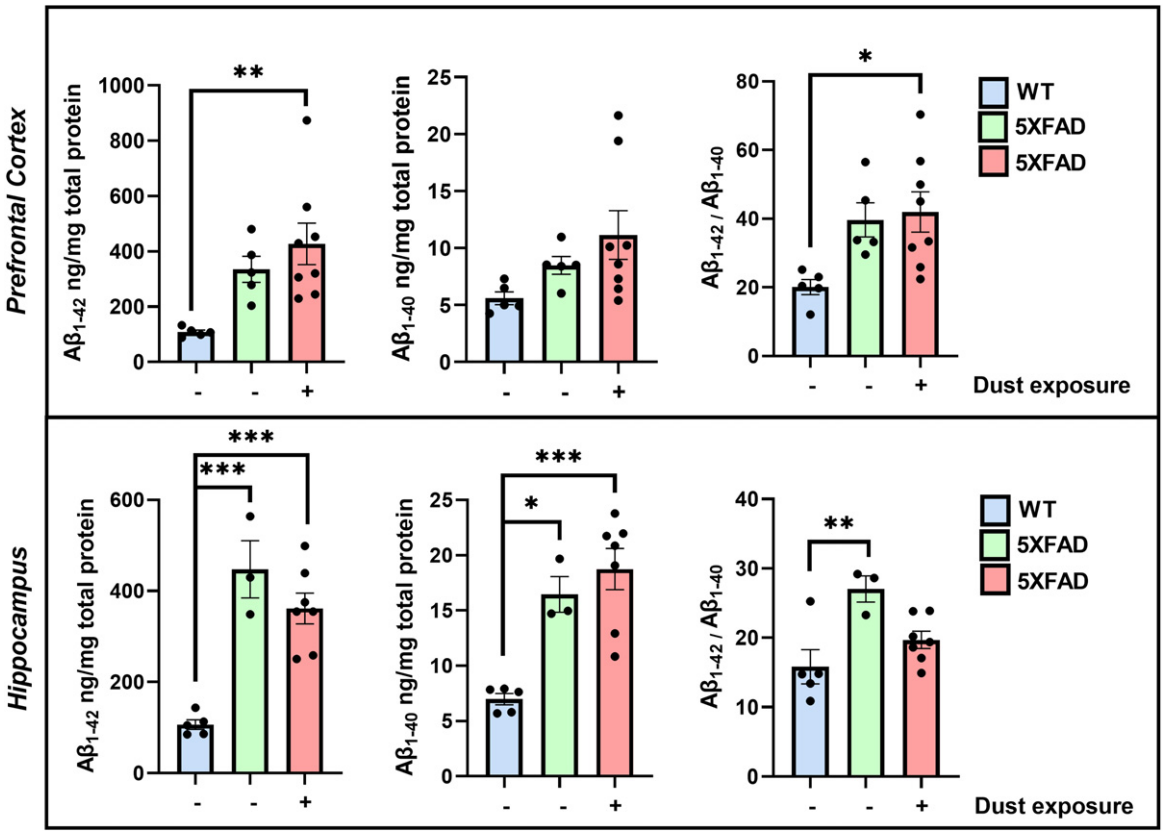

Fig. 2. ELISA analysis for Aβ levels in the prefrontal cortex and hippocampus, in 6-7-month-old WT and 5XFAD mice. Panels for $A\beta_{1-42}$, $A\beta_{1-40}$, and the ratio of $A\beta_{1-42/1-40}$ are shown for the prefrontal cortex and hippocampus. A statistically significant increase in the ratio $A\beta_{1-42}$, $A\beta_{1-40}$ in non-exposed 5XFAD mice compared to non-exposed WT in the hippocampus (mean ± S.E.M: WT – dust: 15.82 ± 2.46; 5XFAD – dust: 30.58 ± 1.67; $^{***}p = 0.0004$), but not in the prefrontal cortex (mean ± S.E.M: WT – dust: 20.10 ± 2.22; 5XFAD – dust: 39.67 ± 4.97; ns, $p = 0.073$). Animals exposed to the dust (lowest dose) showed statistically significant differences for $A\beta_{1-42}$, $A\beta_{1-40}$ ratio compared to WT non-exposed only in the prefrontal cortex (mean ± S.E.M: 5XFAD + dust: 41.95 ± 5.85; WT – dust versus 5XFAD + dust: $^{*}p = 0.025$). However, no effect of dust exposure was observed in the hippocampus compared to WT – dust (mean ± S.E.M: 5XFAD + dust: 19.70 ± 1.25; WT – dust versus 5XFAD + dust: ns, $p = 0.286$). No differences were observed in 5XFAD non-exposed and exposed to dust in either brain region (prefrontal cortex: ns, $p = 0.948$; hippocampus: ns, $p = 0.061$).

differentially distributed in the prefrontal cortex and hippocampal formation.

WTC dust elevates the levels of Chromium in the mouse brain following exposure

Previous studies have investigated the composition of WTCPM [5–8]. Here, we hypothesized that certain chemical elements in the WTCPM may accumulate in the CNS, leading to cognitive decline and exacerbation of AD-type Aβ neuropathology. In this study, WTCPM was instilled via the nares at a dose of 125 μg/50 μl for 3 consecutive days, repeated for 3 weeks, and examined via ICP-MS. After two weeks post-last exposure, animals were sacrificed, and the brains were collected for chemical elements analysis. Only NE and high-exposed (HE) animals were used for these studies. The ICP-MS analysis provided concentrations (ng/mg wet brain tissue) for 32 chemical elements (Table 1).

Most of the chemical elements investigated in connection with AD neurotoxicity include the essential metals iron, copper, zinc, manganese, selenium, and chromium, and the non-essential metals lead, mercury, and aluminum [26, 27]. Among the 32 chemical elements analyzed we found that the concentration of chromium shows a statistically significant 20% increase in the whole brain of 5XFAD mice exposed to a high level of WTCPM compared to vehicle-exposed 5XFAD controls ($^{*}p = 0.02$) (Table 1). No significant detection of the chemical elements was found in WT groups. We want to point out, that the levels of metal detectability are complex due to the variable efflux rates from the brain of many of

Table 1
Concentration (ng/mg) of the 32 chemical elements measured by ICP-MS analysis in WT and 5XFAD Control (Non-Exposed) and Exposed (High Exposure) to the WTC dust mouse brains

Elements	WT			5XFAD		
	Control	Dust Exposure	*p*	Control	Dust Exposure	*p*
P	3828 ± 1032	5047 ± 650	0.34	3985 ± 110	3872 ± 45	0.36
S	2229 ± 486	2600 ± 253	0.51	2527 ± 209	2385 ± 78	0.54
Mg	221 ± 58	229 ± 29	0.91	181 ± 5	174 ± 1	0.17
Ca	189 ± 55	271 ± 177	0.67	230 ± 88	157 ± 43	0.47
Zn	96 ± 73	22 ± 3	0.33	20 ± 2	15.7 ± 0.3	0.05
Fe	30 ± 10	27 ± 3	0.78	22 ± 1	21.3 ± 0.6	0.50
Al	12 ± 6	7.9 ± 2.1	0.55	5.5 ± 1.1	4.7 ± 0.9	0.59
Cu	9.6 ± 3.6	7.4 ± 1.1	0.57	7.6 ± 1.5	5.04 ± 0.09	0.12
Rb	2.9 ± 0.9	4.0 ± 0.5	0.30	3.0 ± 0.1	2.99 ± 0.04	0.79
Se	2.5 ± 1.1	42.0 ± 40.8	0.36	12.4 ± 8.7	9.29 ± 8.15	0.80
Mn	1.6 ± 1.0	0.63 ± 0.07	0.37	0.57 ± 0.03	0.52 ± 0.01	0.17
Ni	1.1 ± 0.5	0.83 ± 0.16	0.61	0.84 ± 0.30	0.32 ± 0.04	0.12
Ba	0.7 ± 0.4	0.06 ± 0.01	0.18	0.06 ± 0.01	0.04 ± 0.00	0.08
As	0.6 ± 0.4	5.1 ± 4.9	0.38	3.62 ± 2.63	2.66 ± 2.30	0.79
Sr	0.5 ± 0.4	0.10 ± 0.04	0.35	0.10 ± 0.02	0.06 ± 0.01	0.16
Sn	0.27 ± 0.06	0.33 ± 0.10	0.63	0.17 ± 0.04	0.12 ± 0.02	0.24
Cd	0.16 ± 0.15	0.00 ± 0.00	0.32	0.01 ± 0.00	0.00 ± 0.00	0.13
Ti	0.15 ± 0.12	0.03 ± 0.00	0.35	0.04 ± 0.01	0.04 ± 0.01	0.69
Cr	0.10 ± 0.01	0.10 ± 0.01	0.43	0.09 ± 0.01	0.11 ± 0.00	0.02*
Mo	0.08 ± 0.02	0.10 ± 0.02	0.50	0.06 ± 0.00	0.06 ± 0.00	0.78
Ag	0.07 ± 0.03	0.05 ± 0.02	0.62	0.08 ± 0.02	0.06 ± 0.00	0.11
Li	0.06 ± 0.01	0.05 ± 0.01	0.46	0.05 ± 0.01	0.04 ± 0.00	0.35
Pb	0.04 ± 0.01	0.05 ± 0.01	0.76	0.02 ± 0.01	0.03 ± 0.02	0.65
V	0.04 ± 0.03	0.01 ± 0.00	0.31	0.01 ± 0.00	0.00 ± 0.00	0.11
Co	0.04 ± 0.02	0.02 ± 0.00	0.40	0.02 ± 0.00	0.01 ± 0.00	0.47
Cs	0.03 ± 0.01	0.03 ± 0.01	0.89	0.05 ± 0.01	0.04 ± 0.00	0.42
U	0.02 ± 0.02	0.00 ± 0.00	0.31	0.00 ± 0.00	0.00 ± 0.00	0.49
Sb	0.01 ± 0.00	0.02 ± 0.01	0.49	0.01 ± 0.00	0.00 ± 0.00	0.82
Be	0.01 ± 0.00	0.01 ± 0.00	0.96	0.00 ± 0.00	0.00 ± 0.00	0.23
La	0.01 ± 0.01	0.00 ± 0.00	0.32	0.00 ± 0.00	0.00 ± 0.00	0.89
Tl	0.00 ± 0.00	0.00 ± 0.00	0.78	0.00 ± 0.00	0.00 ± 0.00	0.79
Bi	0.00 ± 0.00	0.00 ± 0.00	0.51	0.00 ± 0.00	0.00 ± 0.00	0.47

Mean ± S.E.M is shown for each chemical element. *Significant, after correction for multiple testing.

these chemical elements present in the WTCPM. Furthermore, very low concentrations (parts per trillion, PPT), dose, and time dependency exert a major role in detection.

WTC dust affects the transcriptional phenotype in the peripheral immune system

Exposure to WTCPM has multiple deleterious effects on the function of the body, including inducing inflammation. Indeed, exposure to WTCPM has been shown to cause airway inflammation and endothelial dysfunction in the cardiovascular system, with noted increases in polymorphonuclear neutrophils in nasal and bronchoalveolar lavage fluid [23].

Here, we analyzed the peripheral effects on the transcription of immunologically related genes, following WTCPM HE in 5XFAD mice using a Nanostring nCounter Mouse Immunology Transcriptomic Panel (XT-CSO-MNROP1-12). A total of 22 genes were differentially expressed (21 upregulated, 1 downregulated) and are depicted in red in Fig. 3A. Of note, we observed significant increases in the transcription of immunologically related genes including Tumor necrosis factor (*Tnf*), Tumor necrosis factor receptor superfamily 1β (*Tnfrsf1β*), Chemokine (C-C motif) ligand 3 (*Ccl3*; also known as macrophage inflammatory protein 1-alpha), Macrophage scavenger receptor 1 (*Msr1*), and CCAAT-Enhancer Binding Protein β (*Cebpβ*). In addition to differential gene expression, Cell Scores were calculated in nCounter. A trending increase in neutrophils, the granulocytes of the innate immune system, was also noted in the peripheral blood of WTCPM-exposed 5XFAD mice, compared to 5XFAD mice exposed to saline vehicle (Fig. 3B).

Finally, resultant effects on canonical cellular pathways were assessed with IPA. Significant activa-

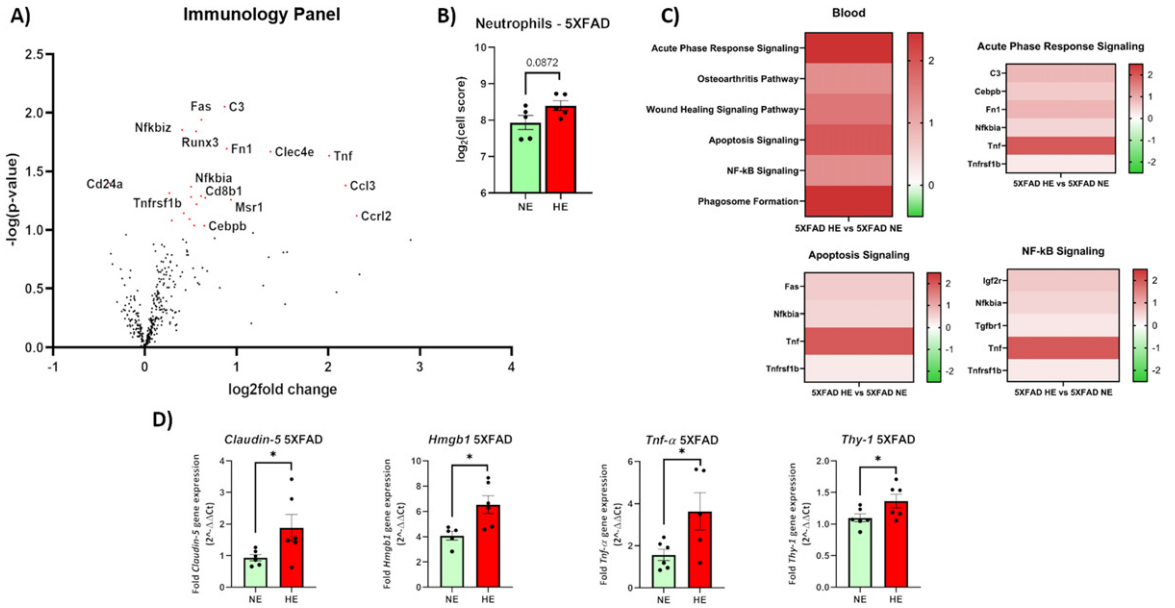

Fig. 3. Transcriptomic analysis in the blood of WTCPM-exposed 5XFAD mice. Volcano plot depicting significantly differentially expressed genes in 5XFAD mice exposed to WTCPM. Genes where $p < 0.05$ are depicted in red. The top 10 genes as identified by the absolute value of log2fold change are labeled (A). Populations of neutrophils in 5XFAD mice exposed to WTCPM increase, as assessed by Log_2(Cell Score) by Nanostring nSolver (B). Ingenuity pathway analysis revealed significant activation of inflammatory-related pathways. Significant pathways were characterized by $p < 0.05$, and $-1.5 < Z < +1.5$ (C). Differentially expressed genes found in top activated pathways (C). *Claudin-5*, *Hmgb1*, *Tnf*-α, and *Thy-1* genes are significantly upregulated in the blood of 5XFAD mice following exposure to WTCPM (D). For a, $^{*}p < 0.05$, $^{**}p < 0.01$ by Student's *t*-test, with Welch's correction.

tion was observed in pathways with an overarching theme of inflammation and included the acute phase response signaling, apoptosis signaling, and NF-κβ signaling (Fig. 3C). Full gene lists indicating genes and differential expression are included in Supplementary Figure 1. Expression of some me of the genes found of interest was analyzed by RTqPCR studies, where *Claudin-5*, High mobility group box 1 (*Hmgb1*), *TNF*-α, and Thy-1 cell surface antigen (*Thy-1)* were upregulated (Fig. 3D).

WTC dust exacerbates the neuroinflammatory transcriptional profile in mouse brain

Based on our evidence and the clinical investigations suggesting that acute exposure to WTCPM may trigger generalized immune inflammatory cascades possibly underlying the collective pathophysiology being experienced by FR following exposure to WTCPM [21], we next explored transcriptional changes in the brain.

To assess transcriptional changes in the brain, hippocampal RNA from 5XFAD mice exposed to high levels of WTCPM and 5XFAD vehicle controls were analyzed with a Nanostring nCounter Mouse Neuropathology Panel (XT-CSO-MNROP1-12), which assesses the transcriptional activity of 770 genes associated with neurodegeneration and neurodegenerative processes. Examination of the transcriptional effects in the hippocampal formation of 5XFAD mice exposed to WTC dust revealed a total of 133 upregulated and 61 downregulated genes, relative to the vehicle-exposed group. Differentially regulated genes ($p < 0.05$) are depicted in red in Fig. 4A. The 10 most differentially expressed genes, as identified by the log2fold change, are depicted in red and labeled in Fig. 4A.

Analysis of cell populations by Nanostring cell score was calculated as the average log [1] scale expression of characteristic genes for specific cell populations, as identified by Nanostring. Levels of astrocytes, endothelial cells, oligodendrocytes, and microglia in the hippocampus of highly-exposed 5XFAD mice were seen to be significantly increased, compared to the vehicle-treated group (Fig. 4B).

Next, using IPA for changes in canonical pathways (log2fold changes) we investigated the resultant biological effects of the transcriptional differences observed in response to WTCPM treatment. A significance threshold of $p < 0.05$ was established *a*

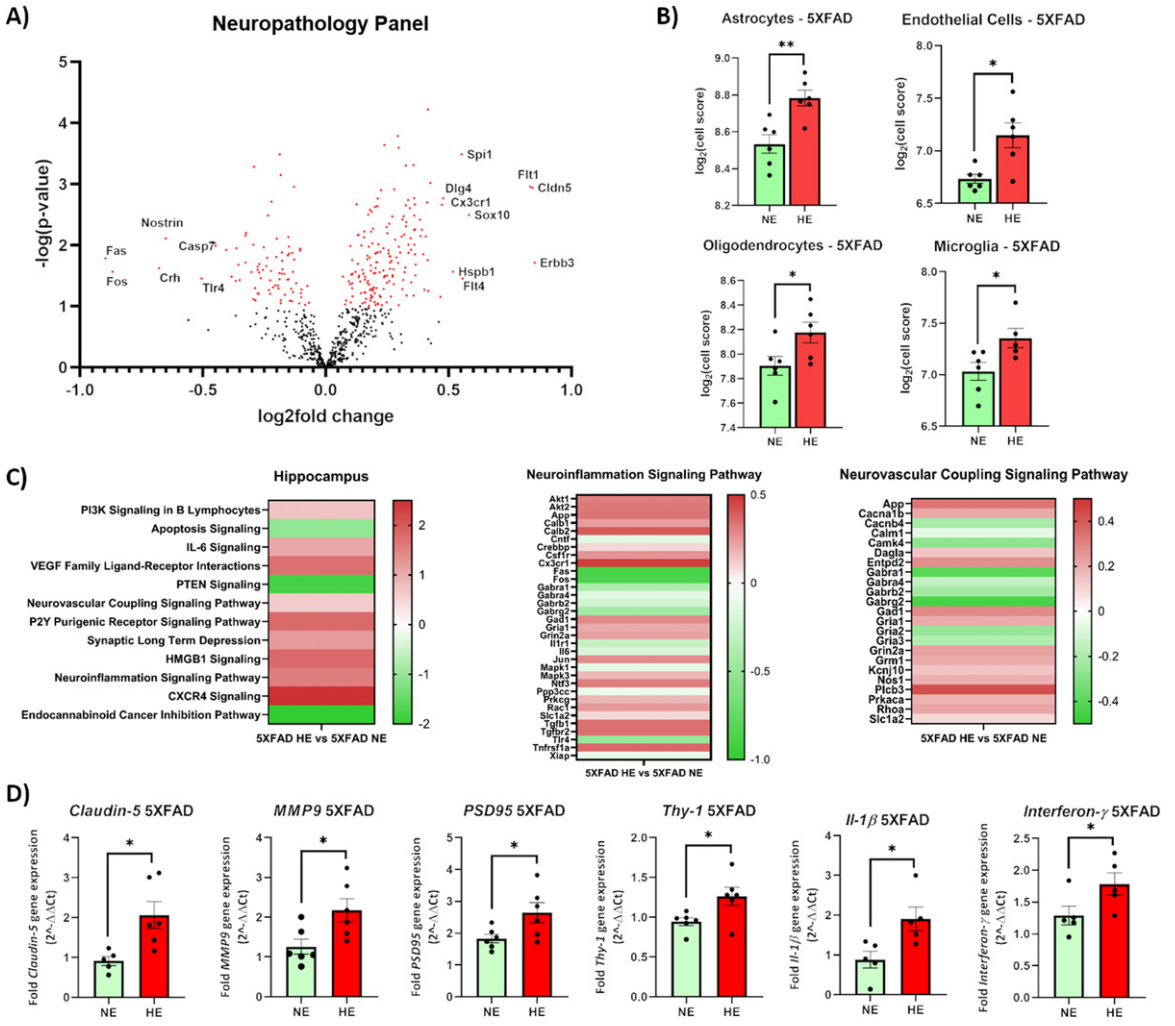

Fig. 4. Transcriptomic analysis in mouse brain. Volcano plot depicting significantly differentially expressed genes in the hippocampus of 5XFAD mice exposed to WTCPM. Genes where $p < 0.05$ are depicted in red. The top upregulated genes as identified by the absolute value of log2fold change are labeled (A). Populations of astrocytes, endothelial cells, oligodendrocytes, and microglia significantly increase in the hippocampus of 5XFAD mice exposed to WTCPM, as assessed by Log_2(Cell Score) by Nanostring nSolver (B). Ingenuity pathway analysis revealed significant activation of inflammatory-related pathways (C). Significant pathways were characterized by $p < 0.05$, and $-1.5 < Z < +1.5$. *Claudin-5*, *Mmp-9*, *PSD95, Thy-1, Il-1*β*, and Interferon-*γ genes are significantly upregulated in the hippocampus of 5XFAD mice following exposure to WTCPM (D). For a, $^{*}p < 0.05$, $^{**}p < 0.01$ by Student's *t*-test, with Welch's correction.

priori to determine canonical pathway enrichment. To quantify activation and repression of pathways, a Z-score threshold of $-1.5 > Z < 1.5$ was chosen a priori. The top 20 differentially activated pathways, as identified by the absolute value of the Z-score, are depicted in Fig. 4C. Exposure to WTC dusts evoked a variety of perturbations in immune function, cell signaling, and homeostatic functioning. Significant activation of immune-related pathways, including Sphingosine-1-phosphate Signaling, Leukocyte Extravasation Signaling, Integrin Signaling, and CXCR4 Signaling were noted in 5XFAD HE mice, compared to the vehicle-treated group. Significant changes in expression of genes involved in the BBB integrity including Claudin-5 (*Cldn5*), Vascular endothelial growth factor A (*Vegfa*), integrin subunit alpha m (*Itgam*), *Thy-1*, C-X3-C motif chemokine receptor 1 (*Cx3cr1*) were found. Full gene lists indicating genes and differential expression are included in Supplementary Figure 2. Differential gene expression was validated by RTqPCR confirming upregulation of *Claudin-5*, *MMP-9* (a matrix metalloproteinase), PSD95, Thy-1, Il-1β, and Interferon-γ (Fig. 4D).

These effects are indicative of a peripherally mounted innate immune response, which might synergistically propagate neuroinflammation. While we did not examine the concentration of chemical elements in circulation, it is possible that the exposure to WTCPM might have exerted peripheral immune responses ultimately resulting in the disruption of brain endothelial tight junction proteins leading to a permissive vascular permeability for migration of peripheral immune modulators to the brain.

DISCUSSION

Emerging evidence has highlighted the importance of investigating the pathophysiology of brain function impairment due to the chronic inhalation of WTCPM, as observed in FR over the years after 9/11. Previous reports have indicated the rise of mental health issues such as depression or anxiety in this population [28, 29]. Here, we investigated the effects of IN exposure to WTC dust in WT and 5XFAD mice, on cognitive decline progression as also the impact of the dust on the regulation of different genes in the peripheral immune and CNS. Previous *in vivo* studies using WT 8-10-week-old mice, treated either acutely with a single dose of 1 mg or a 10-exposures treatment of 63 μg/dose, reported an increase in anxiety-like behavior [24]. In this study, we found that 5XFAD female mice highly exposed to the WTCPM (125 μg/dose × 9 doses) developed a behavior phenotype defined by loss of short- and long-term memory compared to those non-exposed. Moreover, both WT and 5XFAD animals also depicted cognitive decline in spatial working short-term memory. Overall, 5XFAD mice showed more susceptibility to the impact of WTCPM, worsening and accelerating the cognitive decline process. The results of these studies show that mice genetically modified to develop AD-type cognitive deterioration and neuropathology are in agreement with the evidence suggesting that WTCPM exposure is associated with a high risk to develop cognitive deterioration in FR [19].

One of the hallmarks in the neuropathology of AD is the aggregation and clearance Aβ [30]. Interestingly, the WTCPM dust exposure in 5XFAD animals increased the ratio $A\beta_{1\text{-}42/1\text{-}40}$ selectively in the prefrontal cortex but not in the hippocampal formation. The differential brain distribution of the $A\beta_{1\text{-}42/1\text{-}40}$ ratio might occur since the prefrontal cortex is located in the vicinity of the olfactory bulb, and this area is first affected following intranasal instillation of WTCPM. It is well described that the $A\beta_{1\text{-}42}$ is the most toxic fibrillogenic peptide and the main component present in the AD Aβ plaques [31]. Furthermore, a recent study suggests the correlation of soluble $A\beta_{1\text{-}42}$ with cognitive impairment rather than amyloid plaques in familial and sporadic AD [32]. Nevertheless, further studies should be pursued to investigate in depth the AD-Aβ pathology in those FR exposed to the WTC dust.

After demonstrating the detrimental effect of WTCPM exposure on cognition and Aβ levels in our mouse model of WTCPM exposure, we next examined whether different components of the dust, previously characterized by several groups, were present in the brain of those mice exposed to the highest dose. Our ICP-MS data indicate an increased presence of chromium in the brain tissue of WTCPM-exposed mice. There is evidence suggesting that chromium preferentially accumulates in the pituitary gland in and cerebral cortex in rodent models of neurotoxins exposure [33, 34]. This chemical element could enter the brain through the olfactory bulb, which is unprotected by the BBB [35]. For example, we note that a recent study reveals that chromium exposure increases the risk of AD [27]. Lastly, Hegazy et al. [36] reported that rodents exposed intranasally to different concentrations of chromium (0.125, 0.25, 0.5 mg Cr/kg/day) are neurologically impaired including cognitive deterioration and motor functions. Chromium is the most soluble heavy metal, and its high solubility might be one reason we specifically detected it our WTCPM animal model.

Direct toxicity from WTCPM dust has been demonstrated *in vivo*, mainly in the respiratory and circulatory systems [11, 13]. *In vitro*, THP-1 macrophages exposed to WTC dust elicited the production of reactive nitrogen species and correlated directly with cytotoxicity [23]. The same study revealed significant polymorphonuclear neutrophil infiltrate into the bronchoalveolar lavage fluid and an increase of pro-inflammatory cytokines using mice treated with WTC dust. These previously published data alert of the potential toxicity and activation of the peripheral immune system for its potential impact on FR neuroinflammation as discussed below.

Based on this hypothesis, we further examined the effect of acute exposure to high levels of WTCPM on the peripheral immune system of 5XFAD animals. Excitingly we found that among the 21 upregulated genes in peripheral blood, there were several involved

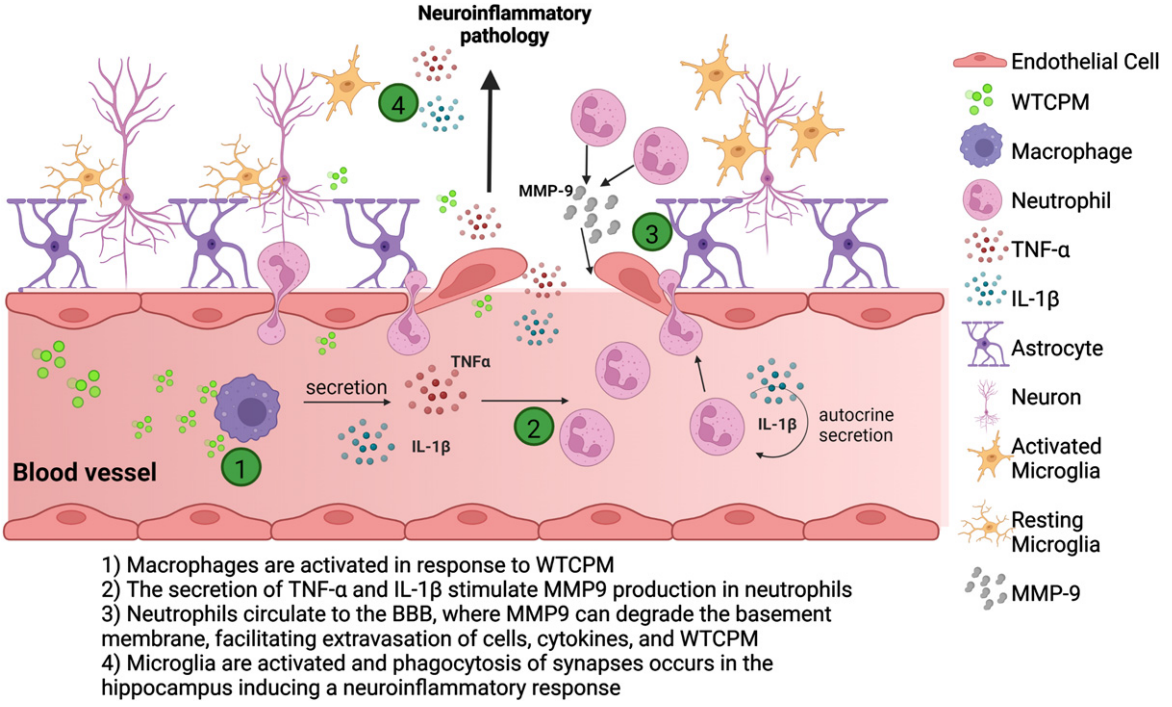

Fig. 5. Scheme of hypothesis. Macrophages, present in the peripheral system, encountering WTCPM, are possibly activated, releasing pro-inflammatory cytokines, including IL-1β, and inducing a subsequent activation of neutrophils. Simultaneously, more signals arise when neutrophils eject IL-1β autocrine release signaling, necessary for early neutrophil recruitment and forward migration from the bloodstream to the BBB. Once the neutrophils reach the extracellular matrix, they produce MMP-9 which exerts a proteolytic activity degrading the different components of the basement membrane, increasing the permeability, and facilitating the infiltration of cells, cytokines, and WTCPM. The neurovascular unit formed by astrocytes, oligodendrocytes, microglia, and endothelial cells along with pericytes, neurons are compromised due to the BBB loss of integrity and function. As a consequence of exposure to the dust, there is an amplification of the neutrophil inflammatory response, by the recruitment of other immune cells such as monocytes and macrophages that will produce cytokines to further perpetuate the pro-inflammatory cascade, leading to the activation of microglia, and ultimately to neuroinflammatory pathology in the brain.

in the immune inflammatory response including *Tnfrsf1β* or *Tnf-α*. High levels of the *Tnf-α* gene were confirmed by RT qPCR along with *Claudin-5*, *Hmgb1*, and *Thy-1*.

We note that TNF-α has been shown to activate NF-κβ signaling, leading to MMP-9 upregulation [37, 38]. Luo et al. [39], demonstrated that *Cebpβ*–upregulated in our studies—binds to the promoter region of MMP-9. For example, MMPs, including MMP-9, exert proteolytic activity capable of degrading various components of the extracellular matrix leading to BBB disruption after focal stroke in rats [40]. MMP-9 is essential for neutrophil migration to the vessels, where they degrade the extracellular matrix, leading to BBB permeability [41]. This is highly relevant to this study since FR may be at are high risk for cerebrovascular disorders which is also a risk factor for cognitive deterioration [42].

It has been reported that neutrophils, key regulators of the innate immune system, mediate recruitment activation and infiltration in the BBB by the release of IL-1β from neutrophils or other immune cells like macrophages [43]. This is consistent with the evidence that WTCPM exposure in rodents promotes an increase in polymorphonuclear neutrophils in nasal and bronchoalveolar lavage fluid [23] in agreement with the trend increase we found in the periphery in our study. This evidence is consistent with a peripherally mounted innate immune response to WTCPM dust exposure, which we hypothesize will synergistically propagate neuroinflammation to the brain.

To better define the impact of WTCPM exposure on the crosstalk between the peripheral immune system and the CNS, we next examined the transcriptomic profile in the hippocampus of 5XFAD mice following exposure to WTC dust. We found, that in the hippocampal formation of 5XFAD mice exposed to WTCPM dust, *Claudin-5* is the most highly upregulated gene. *Claudin-5* serves an essential role in the permeability of the BBB and is highly expressed

in endothelial blood vessels in the brain [44]. It has been reported decreased levels of claudin-5 in the hippocampus of AD mice [45], therefore further investigation would be crucial to determine whether the increase of *Claudin-5* expression in our study may serve as a compensatory mechanism to protect BBB integrity.

This study presents a few limitations. For example, it is worth acknowledging that for these studies only female animals were used. Even though the risk to develop AD is more pronounced in females, both genders should be taken into consideration to ensure rigor and reproducibility to test the hypothesis that exposure to WTCPM causes neurological impairment.

It is well-known that there is a correlation between inflammation and Aβ-tau pathology in AD [46]. Microglia are key in clearing Aβ fibrils, acting as the first line of defense in the early stages of AD [47]. However, when a sustained activation of microglia occurs, they are overcome by Aβ load and tau hyperphosphorylation in the brain, leading to the recruitment of peripheral macrophages, in an attempt to phagocytose the Aβ plaques, the release of pro-inflammatory cytokines, and eventually to neuroinflammation [48]. Hence, it is of paramount importance that future studies examine Aβ and tau neuropathology components to explore possible correlations with cognitive decline and neuroinflammation to further understand the potential impact of WTC dust in the progression of AD-like neuropathology.

One other limitation is that the effects of WTCPM were evaluated shortly after exposure in our studies while the health consequences of FR were rendered years after the initial exposure. The long-term consequences of these initial alterations observed in our studies should be extended accordingly.

In short, as a consequence of acute exposure to the WTCPM dust, there is an amplification of the macrophages-neutrophils-induced inflammatory response, possibly through a mechanism involving the recruitment of other immune cells such as monocytes and macrophages that will continue to produce cytokines to further perpetuate the pro-inflammatory cascade in the periphery. We hypothesize this being a pivotal mechanism through peripheral immune inflammatory changes may feedforward a vicious cycle of immune-inflammatory changes in the brain ultimately leading to the activation of inflammatory microglia and degenerative neuroinflammation (Fig. 5).

Collectively our study provides valuable information relevant to the health of the FR and opens a new horizon for new layouts to understand the impact that acute exposure to WTCPM has on the accelerated onset of AD and other forms of dementia in FR reaching old age.

ACKNOWLEDGMENTS

The authors would also like to acknowledge the following persons for their courageous task of collecting WTC dust on September 12 and 13 near Ground Zero. The field team was led by Dr. Mitchell Cohen and consisted of: M Blaustein, SI Hsu, J Duffey, J Clemente, K Schermerhorn, G Chee, C Prophete, and J Gorczynski. The authors would also like to thank Vassili Tchaikovsky for his technical assistance, and Susan Gursahai for her impeccable work with administrative duties.

The research was supported by Unrestricted Funds and Altschul Foundation. The contents are solely the responsibility of the authors and do not necessarily represent the official views of the NCCIH, NIA, ODS, and NIH.

Authors' disclosures available online (https://www.j-alz.com/manuscript-disclosures/22-1046r1).

SUPPLEMENTARY MATERIAL

The supplementary material is available in the electronic version of this article: https://dx.doi.org/10.3233/JAD-221046.

REFERENCES

[1] Santiago-Colón A, Daniels R, Reissman D, Anderson K, Calvert G, Caplan A, Carreón T, Katruska A, Kubale T, Liu R, Nembhard R, Robison WA, Yiin J, Howard J (2020) World Trade Center Health Program: First decade of research. *Int J Environ Res Public Health* **17**, 7290.

[2] McGee JK, Chen LC, Cohen MD, Chee G, Prophete C, Haykal-Coates N, Wasson SJ, Conner TL, Costa DL, Gavett SH (2003) Chemical analysis of World Trade Center fine particulate matter for use in toxicologic assessment. *Environ Health Perspect* **111**, 972-980.

[3] Vaughan J, Garrett B, Prophete C, Horton L, Sisco M, Soukup JM, Zelikoff JT, Ghio A, Peltier RE, Asgharian B, Lung-chi C, Cohen MDA (2014) novel system to generate WTC dust particles for inhalation exposures. *J Expo Sci Environ Epidemiol* **24**, 105-112.

[4] Cohen MD, Vaughan JM, Garrett B, Prophete C, Horton L, Sisco M, Ghio A, Zelikoff J, Lung-chi C (2015) Impact of acute exposure to WTC dust on ciliated and goblet cells in lungs of rats. *Inhal Toxicol* **27**, 354-361.

[5] Lioy PJ, Weisel CP, Millette JR, Eisenreich S, Vallero D, Offenberg J, Buckley B, Turpin B, Zhong M, Cohen MD,

Prophete C, Yang I, Stiles R, Chee G, Johnson W, Porcja R, Alimokhtari S, Hale RC, Weschler C, Chen LC (2002) Characterization of the dust/smoke aerosol that settled east of the World Trade Center (WTC) in lower Manhattan after the collapse of the WTC 11 September 2001. *Environ Health Perspect* **110**, 703-714.

[6] Lioy PJ, Freeman NC, Millette JR (2002b) Dust: A metric for use in residential and building exposure assessment and source characterization. *Environ Health Perspect* **110**, 969-983.

[7] Gavett SH, Haykal-Coates N, Highfill JW, Ledbetter AD, Chen LC, Cohen MD, Harkema HR, Wagner JG, Costa DL (2003) World Trade Center fine particulate matter causes respiratory tract hyper-responsiveness in mice. *Environ Health Perspect* **111**, 981-991.

[8] Offenberg JH, Eisenreich SJ, Chen LC, Cohen MD, Chee G, Prophete C, Weisel C, Lioy P (2003) Persistent organic pollutants in the dusts that settled across Lower Manhattan after 11 September 2001. *Environ Sci Technol* **37**, 502-508.

[9] González-Maciel A, Reynoso-Robles R, Torres-Jardón R, Mukherjee PS, Calderón-Garcidueñas L (2017) Combustion-derived nanoparticles in key brain target cells and organelles in young urbanites: Culprit hidden in plain sight in Alzheimer's disease development. *J Alzheimers Dis* **59**, 189-208.

[10] Sloan NL, Shapiro MZ, Sabra A, Dasaro CR, Crane MA, Harrison DJ, Luft BJ, Moline JM, Udasin IG, Todd AC, Teitelbaum SL (2021) Cardiovascular disease in the World Trade Center Health Program General Responder Cohort. *Am J Ind Med* **64**, 97-107.

[11] Cohen HW, Zeig-Owens R, Joe C, Hall CB, Webber MP, Weiden MD, Cleven KL, Jaber N, Skerker M, Yip J, Schwartz T, Prezant DJ (2019) Long-term cardiovascular disease risk among firefighters after the World Trade Center disaster. *JAMA Netw Open* **2**, e199775.

[12] Antao VC, Pallos LL, Graham SL, Shim YK, Sapp JH, Lewis B, Bullard S, Alper HE, Cone JE, Farfel MR, Brackbill RM (2019) 9/11 residential exposures: The impact of World Trade Center dust on respiratory outcomes of lower Manhattan residents. *Int J Environ Res Public Health* **16**, 798.

[13] Liu C, Putman B, Singh A, Zeig-Owens R, Hall CB, Schwartz T, Webber MP, Cohen HW, Fazzari MJ, Prezant DJ, Weiden MD (2019) Abnormalities on chest computed tomography and lung function following an intense dust exposure: A 17-year longitudinal study. *Int J Environ Res Public Health* **16**, 1655.

[14] De la Hoz RE, Shapiro M, Nolan A, Celedón JC, Szeinuk J, Lucchini RG (2020) Association of low FVC spirometric pattern with WTC occupational exposures. *Respir Med* **170**, 106058.

[15] Durmus N, Pehlivan S, Zhang Y, Shao Y, Arslan AA, Corona R, Henderson I, Sterman DH, Reibman J (2021) Lung cancer characteristics in the World Trade Center Environmental Health Center. *Int J Environ Res Public Health* **18**, 2689.

[16] Kritikos M, Gandy SE, Meliker JR, Luft BJ, Clouston SAP (2020) Acute versus chronic exposures to inhaled particulate matter and neurocognitive dysfunction: Pathways to Alzheimer's disease or a related dementia. *J Alzheimers Dis* **78**, 871-886.

[17] Clouston SAP, Guralnik JM, Kotov R, Bromet EJ, Luft BJ (2017a) Functional limitations among responders to the World Trade Center attacks 14 years after the disaster: Implications of chronic posttraumatic stress disorder. *J Trauma Stress* **30**, 443-452.

[18] Sweeney MD, Sagare AP, Zlokovic BV (2018) Blood-brain barrier breakdown in Alzheimer disease and other neurodegenerative disorders. *Nat Rev Neurol* **14**, 133-150.

[19] Gong M, Jia J (2022) Contribution of blood-brain barrier-related blood-borne factors for Alzheimer's disease vs. vascular dementia diagnosis: A pilot study. *Front Neurosci* **16**, 949129.

[20] Clouston SAP, Diminich ED, Kotov R, Pietrzak RH, Richards M, Spiro A 3rd, Deri Y, Carr M, Yang X, Gandy S, Sano M, Bromet EJ, Luft BJ (2019) Incidence of mild cognitive impairment in World Trade Center responders: Long-term consequences of re-experiencing the events on 9/11/2001. *Alzheimers Dement (Amst)* **11**, 628-636.

[21] Clouston SAP, Deri Y, Diminich E, Kew R, Kotov R, Stewart C, Yang X, Gandy S, Sano M, Bromet EJ, Luft BJ (2019) Posttraumatic stress disorder and total amyloid burden and amyloid-β 42/40 ratios in plasma: Results from a pilot study of World Trade Center responders. *Alzheimers Dement (Amst)* **11**, 216-220.

[22] Wang S, Lai X, Deng Y, Song Y (2020) Correlation between mouse age and human age in anti-tumor research: Significance and method establishment. *Life Sci* **242**, 117242.

[23] Hernández M, Harrington A, Ma Y, Galdanes K, Halzack B, Zhong M, Vaughan J, Sebasco E, Gordon T, Lippmann M, Chen LC (2020) World Trade Center Dust induces airway inflammation while promoting aortic endothelial dysfunction. *Toxicol Appl Pharmacol* **400**, 115041.

[24] Hernández M, Vaughan J, Gordon T, Lippmann M, Gandy S, Chen LC (2022) World Trade Center dust induces nasal and neurological tissue injury while propagating reduced olfaction capabilities and increased anxiety behaviors. *Inhal Toxicol* **34**, 175-188.

[25] Clouston SAP, Pietrzak RH, Kotov R, Richards M, Spiro A 3rd, Scott S, Deri Y, Mukherjee S, Stewart C, Bromet E, Luft BJ (2017) Traumatic exposures, posttraumatic stress disorder, and cognitive functioning in World Trade Center responders. *Alzheimers Dement (NY)* **3**, 593-602.

[26] Strumylaite L, Kregzdyte R, Kucikiene O, Baranauskiene D, Simakauskiene V, Naginiene R, Damuleviciene G, Lesauskaite V, Zemaitiene R (2022) Alzheimer's disease association with metals and metalloids concentration in blood and urine. *Int J Environ Res Public Health* **19**, 7309.

[27] Tanvir Kabir Md T, Uddin Md S, Zaman S, Begum Y, Ashraf Md G, Bin-Jumah MN, Bungau SG, Mousa SA, Abdel-Daim MM (2021) Molecular mechanisms of metal toxicity in the pathogenesis of Alzheimer's disease. *Mol Neurobiol* **58**, 1-20.

[28] Lippmann M, Cohen MD, Chen LC (2015) Health effects of World Trade Center (WTC) Dust: An unprecedented disaster's inadequate risk management. *Crit Rev Toxicol* **45**, 492-530.

[29] Salama A, Hegazy R, Hassan A (2016) Intranasal chromium induces acute brain and lung injuries in rats: Assessment of different potential hazardous effects of environmental and occupational exposure to chromium and introduction of a novel pharmacological and toxicological animal model. *PLoS One* **11**, e0168688.

[30] Masters CL, Bateman R, Blennow K, Rowe CC, Sperling RA, Cummings JL (2015) Alzheimer's disease. *Nat Rev Dis Primers* **1**, 15056.

[31] Hampel H, Hardy J, Blennow K, Chen C, Perry G, Kim SH, Villemagne VL, Aisen P, Vendruscolo M, Iwatsubo T, Masters CL, Cho M, Lannfelt L, Cummings JL, Vergallo A (2021) The amyloid-β pathway in Alzheimer's disease. *Mol Psychiatry* **26**, 5481-5503.

[32] Sturchio A, Dwivedi AK, Malm T, Wood MJA, Cilia R, Sharma JS, Hill EJ, Schneider LS, Graff-Radford NR, Mori H, Nübling G, El Andaloussi S, Svenningsson P, Ezzat K, Espay AJ; Dominantly Inherited Alzheimer Consortia (DIAN) (2022) High soluble amyloid-β42 predicts normal cognition in amyloid-positive individuals with Alzheimer's disease-causing mutations. *J Alzheimers Dis* **90**, 333-348.

[33] North CS, Pollio DE, Hong BA, Pandya A, Smith RP, Pfefferbaum B (2015) The postdisaster prevalence of major depression relative to PTSD in survivors of the 9/11 attacks on the World Trade Center selected from affected workplaces. *Compr Psychiatry* **60**, 119-125.

[34] Jordan HT, Osahan S, Li J, Stein RS, Friedman SM, Brackbill RM, Cone JE, Gwynn C, Mok HK, Farfel MR (2019) Persistent mental and physical health impact of exposure to the September 11, 2001 World Trade Center terrorist attacks. *Environ Health* **18**, 12.

[35] Fan J, Tao W, Li X, Li H, Zhang J, Wei D, Chen Y, Zhang Z (2019) The contribution of genetic factors to cognitive impairment and dementia: Apolipoprotein E gene, gene interactions, and polygenic risk. *Int J Mol Sci* **20**, 1177.

[36] Wise JP Jr, Young JL, Cai J, Cai L (2022) Current understanding of hexavalent chromium [Cr(VI)] neurotoxicity and new perspectives. *Environ Int* **158**, 106877.

[37] Chiu PS, Lai SC (2013) Matrix metalloproteinase-9 leads to claudin-5 degradation via the NF-κB pathway in BALB/c mice with eosinophilic meningoencephalitis caused by Angiostrongylus cantonensis. *PLoS One* **8**, e53370.

[38] Aslam M, Ahmad N, Srivastava R, Hemmer B (2012) TNF-alpha induced NFkappaB signaling and p65 (RelA) overexpression repress Cldn5 promoter in mouse brain endothelial cells. *Cytokine* **57**, 269-275.

[39] Luo BY, Zhou J, Guo D, Yang Q, Tian Q, Cai DP, Zhou RM, Xu ZZ, Wang HJ, Chen SY, Xie WB (2022) Methamphetamine induces thoracic aortic aneurysm/dissection through C/EBPβ. *Biochim Biophys Acta Mol Basis Dis* **1868**, 166447.

[40] Romanic AM, White RF, Arleth AJ, Ohlstein EH, Barone FC (1998) Matrix metalloproteinase expression increases after cerebral focal ischemia in rats: Inhibition of matrix metalloproteinase-9 reduces infarct size. *Stroke* **29**, 1020-1030.

[41] Zou D, Hu W, Qin J, Wei Z, Wang D, Li L (2021) Rapid orderly migration of neutrophils after traumatic brain injury depends on MMP9/13. *Biochem Biophys Res Commun* **579**, 161-167.

[42] Sforza M, Bianchini E, Alivernini D, Salvetti M, Pontieri FE, Sette G (2022) The impact of cerebral vasomotor reactivity on cerebrovascular diseases and cognitive impairment. *J Neural Transm* **129**, 1321-1330.

[43] De Oliveira S, Rosowski EE, Huttenlocher A (2016) Neutrophil migration in infection and wound repair: Going forward in reverse. *Nat Rev Immunol* **16**, 378-391.

[44] Morita K, Sasaki H, Furuse M, Tsukita S (1999) Endothelial claudin: Claudin-5/TMVCF constitutes tight junction strands in endothelial cells. *J Cell Biol* **147**, 185-194.

[45] Zhu N, Wei M, Yuan L, He X, Chen C, Ji A, Zhang G (2022) Claudin-5 relieves cognitive decline in Alzheimer's disease mice through suppression of inhibitory GABAergic neurotransmission. *Aging* **14**, 3554-3568.

[46] Kinney JW, Bemiller SM, Murtishaw AS, Leisgang AM, Salazar AM, Lamb BT (2018) Inflammation as a central mechanism in Alzheimer's disease. *Alzheimers Dement (N Y)* **4**, 575-590.

[47] Chakrabarty P, Jansen-West K, Beccard A, Ceballos-Diaz C, Levites Y, Verbeeck C, Zubair AC, Dickson D, Golde TE, Das P (2010) Massive gliosis induced by interleukin-6 suppresses Abeta deposition in vivo: Evidence against inflammation as a driving force for amyloid deposition. *FASEB J* **24**, 548-559.

[48] Krabbe G, Halle A, Matyash V, Rinnenthal JL, Eom GD, Bernhardt U, Miller KR, Prokop S, Kettenmann H, Heppner FL (2013) Functional impairment of microglia coincides with Beta-amyloid deposition in mice with Alzheimer-like pathology. *PLoS One* **8**, e60921.